Article

J. Biol. Regul. Homeost. Agents. 2024; 38(6): 5125–5136
https://doi.org/10.23812/j.biol.regul.homeost.agents.20243806.409

DUSP5 Protects against Diabetes-Related Heart Failure via Inhibiting *PPARα*-Mediated Fatty Acid Oxidation

Chenliang Qi[1,†], Jianfeng Yin[1,†], Jianxiang Gan[1], Kun Wang[1], Ji Xu[1,*]

[1]Department of Cardiovascular, Affiliated Hospital of Nanjing University of Chinese Medicine, Changzhou Hospital of Traditional Chinese Medicine, 213004 Changzhou, Jiangsu, China
*Correspondence: xuji13775233019@163.com (Ji Xu)
[†]These authors contributed equally.
Submitted: 15 April 2023 Revised: 24 May 2023 Accepted: 13 June 2023 Published: 1 June 2024

Background: Heart failure (HF) is one of the most common complications of diabetes mellitus. This study aimed to investigate the potential roles of dual specificity phosphatase 5 (*DUSP5*), a negative regulator of mitogen-activated protein kinase signaling, in diabetes-related HF.

Methods: Sprague dawley rats were randomly divided into the sham group, streptozotocin (STZ) group, STZ + vector group, STZ + Ad-*DUSP5* group and vehicle group, and a group that was intravenously administered *DUSP5*-nanoparticle (NP) that carried the peroxisome proliferator-activated receptor alpha (*PPARα*) antagonist GW-6471. Triphenyl tetrazolium chloride staining was used to analyze the infarct area. The apoptosis of cardiomyocytes was determined using the terminal deoxynucleotidyl transferase (TdT)-mediated dUTP nick-end labeling assay. For *in vitro* assays, mRNA expression was determined using quantitative reverse transcription-PCR; protein expression was detected using western blotting; protein localization was determined using immunofluorescence assay; and cell apoptosis was analyzed using flow cytometry.

Results: *DUSP5* expression was decreased in patients with diabetes-related HF, as well as in the *in vitro* model ($p < 0.05$). However, overexpression of *DUSP5* inhibited the apoptosis of cardiomyocytes and fatty acid oxidation ($p < 0.05$). Moreover, *DUSP5* mediated the nuclear translocation of *PPARα* ($p < 0.05$). By contrast, overexpression of *PPARα* promoted fatty acid oxidation and the apoptosis of cardiomyocytes ($p < 0.05$). The *in vivo* assay showed that *DUSP5* overexpression inhibited the infarct area and death of cardiomyocytes ($p < 0.05$). Additionally, *DUSP5*-NP that delivered GW-6471 markedly alleviated heart damage induced by diabetes mellitus ($p < 0.05$).

Conclusions: Our findings suggest that *DUSP5* exerts a protective effect on diabetes-related HF by suppressing *PPARα*-dependent fatty acid oxidation. Therefore, *DUSP5* may be a potential target for diabetes-related HF.

Keywords: diabetes-related heart failure; dual specificity phosphatase 5; peroxisome proliferator-activated receptor alpha; fatty acid oxidation; apoptosis

Introduction

Heart failure (HF) is one of the most common types of cardiovascular disease (CVD) [1]. HF is caused by various factors, such as cardiac contractile or diastolic dysfunction [2]. Recently, increasing evidence has reported that HF is one of the most common complications of diabetes mellitus (DM) [3–6]. HF is four times more prevalent in DM patients than in the general population. Diabetes-related HF is a long-term chronic metabolic disorder, frequently induced by the alteration in cardiac fatty acid oxidation (FAO) and glycolysis [7–9]. Notably, uncovering the underlying molecular mechanisms of DM-related HF may catch the Achilles' heel.

An imbalance in mitochondrial energy metabolism is common in CVD [10]. Alterations in mitochondrial FAO and glucose oxidation are closely related to carbohydrate oxidation [11]. Sustained FAO by the mitochondria induces cardiomyocyte dysfunction and affects cardiac efficiency, resulting in impaired heart function in diabetes-related HF [12,13]. Notably, inhibiting FAO regulators, such as peroxisome proliferator-activated receptors (*PPARs*), restores heart functions. *PPARs* are lipid sensors that regulate energy metabolism. *PPARα* modulates the adaptive response to fasting by modulating fatty acid transport, FAO and ketogenesis [14]. However, high levels of *PPARα* are frequently found to be associated with an increase in glycolysis and a decrease in fatty acid catabolism, thus contributing to the accumulation of oxidative stress and cardiomyocyte death [15]. However, the underlying mechanisms are still unclear.

Dual specificity phosphatase 5 (*DUSP5*) is a member of the phosphatase superfamily [16]. *DUSP5* modulates the dephosphorylation of threonine/serine and tyrosine residues [17]. Its dysfunction is associated with various diseases, including cancer, diabetic complications and

Journal of
BIOLOGICAL REGULATORS
and Homeostatic Agents

CVD [18–20]. For example, histone deacetylase 1 suppresses *DUSP5*-mediated dephosphorylation by promoting the acetylation of *DUSP5*, resulting in the pathogenesis of cardiomyocyte hypertrophy [21]. In addition, *DUSP5* inhibits proliferative extracellular signal-regulated kinase 1/2 signaling in the left ventricle [22]. However, the potential of *DUSP5* in diabetes-related HF has not yet been elucidated. This study aimed to investigate the roles of *DUSP5* in diabetes-related HF and the underlying molecular mechanisms. We hypothesized that aberrant levels of *DUSP5* may induce the loss of cardiomyocytes and contribute to the development of diabetes-related HF.

Materials and Methods

Cell Culture and Transfection

AC16 cell lines were obtained from American Type Culture Collection (CRL-3568; Manassas, VA, USA), and the cell line was authenticated to be used in subsequently assays. Cells were cultured in Claycomb medium supplemented with 10% fetal bovine serum (FBS; A5669701; Gibco, Waltham, MA, USA) and 1% penicillin/streptomycin (15070063; Gibco, Waltham, MA, USA), 0.1 mM noradrenaline (Y0000682; Sigma-Aldrich, Darmstadt, Germany), and 2 mM L-glutamine (10564029; Sigma-Aldrich, Darmstadt, Germany) at 37 °C in 5% CO_2. STR identification was performed by Shanghai GuanDao Biological Engineering Co., Ltd (Shanghai, China). The submitted profile is an exact match for the following human cell line(s) in the Cellosaurus STR database (8 core loci plus Amelogenin): AC16.

Cells were exposed to normal glucose (5.55 mmol/L of d-glucose, NG, G5767; Sigma-Aldrich, Darmstadt, Germany) and high glucose (30 mmol/L of d-glucose, HG) for 24 h. Afterwards, cells were treated with PPARα antagonist GW-6471 (50 μM) (ab254317; Abcam, Cambridge, UK), or PPARα agonist WY14643 (200 μM) (ab141142; Abcam, Cambridge, UK) and Fenofibrate (FEN; 10 μM) (ab120832; Abcam, Cambridge, UK).

50 nM of short hairpin (sh)RNA of DUSP5 and the negative control (NC) as well as *DUSP5* overexpression plasmids and its empty vector (GenePharm, Shanghai, China) were mixed with Lipofectamine 2000 (11668019; Thermo Fisher Scientific, Inc., Waltham, MA, USA) for 6 h. Then cells were transfected with the mixture for 48 h. After transfection, cells were used in the following experiment. The sequences of DUSP5 shRNAs were as following: sh*DUSP5* 1#: 5′-GCGTGCCTCCTGATTTCTTTC-3′; sh*DUSP5* 2#: 5′-GGATTTGACTCCAAGTGAATT-3′; sh*NC*: 5′-TTCTCCGAACGTGTCACGT-3′.

Recombinant Adenoviruses Construction

Recombinant adenoviruses expressing rat DUSP5 (Ad-*DUSP5*) complementary DNA (cDNA) were constructed by GenePharm, Shanghai.

Animal Care

This study was approved by the Animal Care Broad of Nanjing Hospital Affiliated to Nanjing Medical University ([2022]027). The procedures of *in vivo* assays were performed in accordance with the Care and Use of Laboratory Animals published by the US National Institutes of Health. Male Sprague Dawley (SD) rats (160–180 g, 14 weeks old; n = 36) were obtained from Experimental Animal Center of Zhejiang Province, China. All rats were housed in moderate temperature (22 ± 2 °C) at the humidity of 50–60%, in a 12-h light/dark cycle, and free access to food and water. The body weight of rats was measured once a week.

Induction of Diabetes-Related HF

Diabetes-related HF was induced as previously described [23,24]. Rats were randomly divided into the sham group, streptozotocin (STZ) (S0130; Sigma-Aldrich, Darmstadt, Germany) group, STZ + vector group, Ad-*DUSP5* group, vehicle group and *DUSP5*-nanoparticles (NP) group. Briefly, rats (n = 36) in the diabetic group were intraperitoneally injected with STZ (30 mg/kg). After 7 days, the rats with a fasting blood glucose over 11.1 mmol/L were deemed diabetic models after consecutive measurements. The rats were then intraperitoneally injected with vector (200 μL of 10^{12} pfu/mL in saline; n = 6), Ad-*DUSP5* (200 μL of 10^{12} pfu/mL in saline; n = 6), vehicle (120 mg/kg/day; n = 6) or *DUSP5*-NP (120 mg/kg/day; n = 6) for 12 weeks. Rats intraperitoneally injected with citrate buffer were used as the blank control group (sham; n = 6). After 12 weeks, all rats were sacrificed by exsanguination under anesthesia with an intraperitoneal injection of 3% sodium pentobarbital (150 mg/kg). The heart tissues were subsequently collected and used in the following experiments.

Triphenyl Tetrazolium Chloride (TTC) Staining

Rats were anesthetized by spontaneous inhalation and were maintained under general anesthesia with 1–2% isoflurane. The rats were then subjected to left coronary artery occlusion for 30 min, followed by 3 h/24 h of reperfusion. Hearts were then excised and stained with TTC to measure the area of necrosis.

Terminal Deoxynucleotidyl Transferase (TdT)-Mediated dUTP Nick-End Labeling (TUNEL) Assay

Paraffin-embedded tissue sections were dewaxed. After hydration, the sections were fixed with 4% paraformaldehyde and permeabilized in 0.1% Triton X-100 (P0096; Beyotime, Shanghai, China). The sections were then cultured with proteinase K for 15 min at 37 °C and 3% H_2O_2 (88597; Sigma-Aldrich, Darmstadt, Germany), and incubated with *in situ* Cell Death Detection Kit (11684795910; Roche, Basel, Switzerland). The sections were counterstained with 4′,6-diamidino-2-phenylindole (DAPI) in the dark. Subsequently, apoptotic cells in the

sections were captured under a microscope (DMiL, Leica, Wetzlar, Germany) and quantified by ImageJ software (ProteinSimple v.3.5.0; Bio-Techne, Minneapolis, MN, USA). The apoptosis rate was calculated as follows: apoptosis rate = TUNEL-positive cells/total cells × 100%.

Mesenchymal Stem Cell (MSC) Isolation

MSCs were obtained from male Sprague-Dawley rats. Following isolation from the bone marrow, MSCs were cultured in Iscove's Modified Dulbecco's Medium (IMDM; 31980030; Invitrogen, Waltham, MA, USA) with 10% FBS (A5669701; Gibco, Waltham, MA, USA) in 5% CO_2 at 37 °C. MSCs at passages 3–4 were pretreated with 1 μmol/L ATV (1044538; Sigma-Aldrich, Darmstadt, Germany.) in exosome-free IMDM for 48 h, after which, the conditioned medium was collected. Images of the MSCs were captured using a light microscope (Leica, Wetzlar, Germany), and flow cytometric analysis was used to detect the MSC-specific surface markers, *CD106*, *CD29*, *CD44* and *CD34* (eBioscience, Waltham, MA, USA).

Exosome Collection and NP Preparation

Rat MSCs, at a confluence of ≥80%, were collected and cultured in FBS-free medium for 48 h. Afterwards, the supernatants were collected, filtered using a polyvinylidene fluoride filter (HVLP04700; Sigma-Aldrich, Darmstadt, Germany) and then ultracentrifuged at 120,000 ×g. Subsequently, the exosomes were identified by transmission electron microscopy (TEM) (Krios G4 Cryo-TEM; Thermo Fisher Scientific, Waltham, MA, USA) and analyzed using nanoparticle tracking analysis (NTA) software (version 2.3; Claisse, Amsterdam, Netherlands). Afterwards, the exosomes were collected and stored at –80 °C within 30 days. The *PPARα* antagonist GW-6471 was provided by Abcam (Cambridge, UK). Subsequently, the exosomes were dissolved, and GW-6471 was loaded in a mini extruder (610020; Sigma-Aldrich, Darmstadt, Germany) with a 100-mm polycarbonate membrane (610007; Sigma-Aldrich, Darmstadt, Germany). Afterwards, the NP were detected and harvested. Subsequently, *DUSP5*-NP were intraperitoneally injected into rats (n = 6) at a dosage of 120 mg/kg/day. DUSP5 exosomes containing vehicle were used as the control treatment.

Reactive Oxygen Species (ROS) and Malondialdehyde (MDA) Determination

Following trypsinization, cells were resuspended and centrifuged. The release of ROS was determined using the Cellular ROS assay kit (ab186027; Abcam, Cambridge, UK) at a wavelength of 590 nm according to the manufacturer's protocols. The release of MDA was determined using the corresponding MDA assay kit (ab238537; Abcam, Cambridge, UK) at a wavelength of 450 nm according to the manufacturer's protocols.

Quantitative Reverse Transcription (qRT)-PCR

Total RNA was collected from AC16 cells and tissues using Trizol reagent (15596018CN, Invitrogen, Waltham, MA, USA). cDNA was synthesized using a PrimeScript® RT Reagent Kit (RR037A; Takara, Shiga, Japan). Quantitative PCR was performed using an SYBR® Premix Ex TaqTM II Kit (RR390A; Takara, Shiga, Japan). Glyceraldehyde-3-phosphate dehydrogenase (*GAPDH*) was used the loading control. Relative mRNA expression of the target genes was calculated with $2^{-\Delta\Delta Ct}$ method. The sequences of the primers used in PCR were as following: *DUSP5*, F: 5′-GCCAGCTTATGACCAGGGTG-3′ and R: 5′-GTCCGTCGGGAGACATTCAG-3′; caveolin 1 (*CAV1*), F: 5′-AATACTGGTTTTACCGCTTGCT-3′ and R: 5′-CATGGTACAACTGCCCAGATG-3′; fatty acid binding protein 4 (*FABP4*), F: 5′-TGGGCCAGGAATTTGACGA-3′ and R: 5′-CATTTCTGCACATGTACCAGGACAC-3′; carnitine palmitoyltransferase 1B (*CPT1B*), F: 5′-CATGTATCGCCGTAAACTGGAC-3′ and R: 5′-TGGTAGGAGCACATAGGCACT-3′; *PPARα*, F: 5′-CGGTGACTTATCCTGTGGTCC-3′ and R: 5′-CCGCAGATTCTACATTCGATGTT-3′; *GAPDH,* F: 5′-TCAAGAAGGTGGTGAAGCAGG-3′ and R: 5′-TCAAAGGTGGAGGAGTGGGT-3′.

Western Blot

Protein was harvested from AC16 cells. Protein concentration was determined using a bicinchoninic acid assay kit (ab102536; Abcam, Cambridge, UK). An equal amount of protein (20 μM) was separated by a 12% sodium dodecyl sulfate-polyacrylamide gel electrophoresis (SDS-PAGE) at 120 V. Then the protein was moved onto PVDF membrane. After sealed with 5% non-fat milk, the membranes were incubated overnight at 4 °C with primary antibodies against DUSP5 (ab200708; 1: 1000, Abcam, Cambridge, UK), PPARα (ab314112; 1: 1000, Abcam, Cambridge, UK), apoptosis-linked gene 2-interacting protein X (ALIX) (ab275377; 1: 1000, Abcam, Cambridge, UK), cluster of differentiation 81 (CD81) (ab109201, 1: 2500; Abcam, Cambridge, UK), histone H3 (H3A) (ab1791; 1: 2000, Abcam, Cambridge, UK), GAPDH (ab9485; 1: 2500, Abcam, Cambridge, UK), and then with goat-anti-rabbit secondary antibodies (ab6721; 1: 5000, Abcam, Cambridge, UK). Finally, the bands were captured using an enhanced chemiluminescence (ECL) kit (ab133406; Abcam, Cambridge, UK). AlphaView 2.0 gel imaging analysis software (ProteinSimple; Bio-Techne, Minneapolis, MN, USA) was used for quantitative analysis.

Immunofluorescence Assay

After transfection, the cells were collected and seeded into a 24-well plate. Afterwards, the cells were fixed with 4% paraformaldehyde and permeabilized in 0.1% Triton X-100. The cells were then washed with 10%

Journal of
BIOLOGICAL REGULATORS
and Homeostatic Agents

phosphate buffered saline (PBS, P4474, Sigma-Aldrich, Darmstadt, Germany). Afterwards, the cells were incubated with primary antibodies against DUSP5 (ab200708, 1:100, Abcam, Cambridge, UK), heat-shock protein 60 (HSP60, ab190828, 1:100, Abcam, Cambridge, UK) and cytochrome C (cyto C, ab133504, 1:100, Abcam, Cambridge, UK). Nuclei were stained with DAPI. Finally, images of the cells were captured using a microscope (Leica, Wetzlar, Germany).

Flow Cytometry

After transfection, the cells were collected and plated in a 24-well plate. The cells were resuspended in Annexin V-fluorescein isothiocyanate (Abcam) in Annexin binding and cultured for 15 min. The cells were then incubated with 0.5 µL propidium iodide (Abcam). The apoptosis rates were analyzed using a FACSCantoII flow cytometer (BD Biosciences, Franklin Lake, NJ, USA) with FlowJo v.10 (BD Biosciences, Franklin Lake, NJ, USA).

Mycoplasma Detection

Mycoplasma detection was performed using quantitative reverse transcription (qRT)-PCR as previously described [25].

Bioinformatics Analysis

Differentially expressed genes (DEGs) in patients with diabetes-mediated HF compared with in healthy controls were analyzed using the online microarray dataset GSE26887. The enrichment of proteins was analyzed using Gene Ontology (GO) and Kyoto Encyclopedia of Genes and Genomes (KEGG).

Statistical Analysis

All data were analyzed using GraphPad Prism v. 9.5.0 (Boston, MA, USA). Data are expressed as the mean ± standard deviation. Each experiment was performed in triplicate. The differences between two groups were analyzed using Student's *t*-test. The differences among multiple groups were evaluated by one-way ANOVA followed by Bonferroni post hoc test. $p < 0.05$ indicated a statistically significant difference.

Results

DUSP5 is Downregulated in Diabetes-Mediated HF

The online microarray GSE26887 was used to analyze the DEGs in diabetes-mediated HF. *DUSP5*, ankyrin repeat domain 2, solute carrier family 7 member 2, etc., were downregulated in patients with diabetes-mediated HF (Fig. 1A). The upregulated genes were enriched in drug metabolism-cytochrome *P450*, *cAMP*-signaling pathway and *PPAR* signaling pathway (Fig. 1B). The downregulated genes were enriched in tumor necrosis factor signaling pathway, *Salmonella* infection, phagosome, lipid and atherosclerosis, cellular senescence, apoptosis, advanced glycation end product (*AGE*)-receptor for *AGE* signaling pathway in diabetic complications, as well as in cell-cell adhesion and inflammation (Fig. 1B). To confirm the roles of *DUSP5* in diabetes-mediated HF, cells were exposed to HG. The results showed that *DUSP5* expression was significantly decreased in cells exposed to HG compared with NG ($p < 0.01$; Fig. 1C,D; **Supplementary Fig. 1**). Moreover, we determined the expression of the mitochondrial function indicators *HSP60* (red) and *cyto C* (green) in the cells exposed to HG. Cells were transfected with *DUSP5* shRNAs or *DUSP5* overexpression plasmids. As shown in **Supplementary Fig. 2**, *DUSP5* expression was markedly increased following transfection with *DUSP5* overexpression plasmids ($p < 0.001$), while it was downregulated by *DUSP5* shRNAs ($p < 0.01$). Notably, *DUSP5* shRNA 1#, which had more marked efficiency ($p < 0.01$), was used in the following experiments. Interestingly, *DUSP5* knockdown markedly inhibited the expression of *HSP60* ($p < 0.05$) and increased *cyto C* expression ($p < 0.001$; Fig. 1E; **Supplementary Fig. 3**). In contrast, *DUSP5* overexpression upregulated *HSP60* ($p < 0.01$) and downregulated *cyto C* ($p < 0.01$; Fig. 1E; **Supplementary Fig. 3**), suggesting that *DUSP5* may maintain mitochondrial function and suppress cardiomyocyte death in diabetes-mediated HF. FAO plays a vital role in maintaining mitochondrial function. Therefore, we determined the expression of FAO regulators. Consistently, *DUSP5* deficiency markedly increased the mRNA expression of caveolin 1 (*CAV1*), fatty acid binding protein 4 (*FABP4*) and carnitine palmitoyltransferase 1B (*CPT1B*) ($p < 0.01$; Fig. 1F), while the expression of *PPARα* showed no significant changes.

DUSP5 Overexpression Suppresses the Death of AC16 Cells

Compared with the positive control, the results of qRT-PCR in AC16 cells showed no amplification (**Supplementary Fig. 4A**), suggesting that AC16 cells were not infected with *Mycoplasma*. AC16 cells were transfected with *DUSP5* overexpression plasmids to further confirm the roles of *DUSP5* in diabetes-mediated HF. We found that the release of ROS and MDA were significantly decreased post-transfection with *DUSP5* overexpression plasmids compared with those in the HG + vector group ($p < 0.05$, $p < 0.01$; Fig. 2A,B). *DUSP5* overexpression also significantly alleviated the death of AC16 cells induced by HG ($p < 0.01$; Fig. 2C).

DUSP5 Suppresses the Nuclear Expression of PPARα

As shown in Fig. 1, we found that the mRNA expression of *PPARα* showed no significant changes. Given that *PPARα* is the transcription factor that regulates fatty acid metabolism, we therefore hypothesized that *DUSP5* may modulate the subcellular localization of *PPARα*. Fig. 3

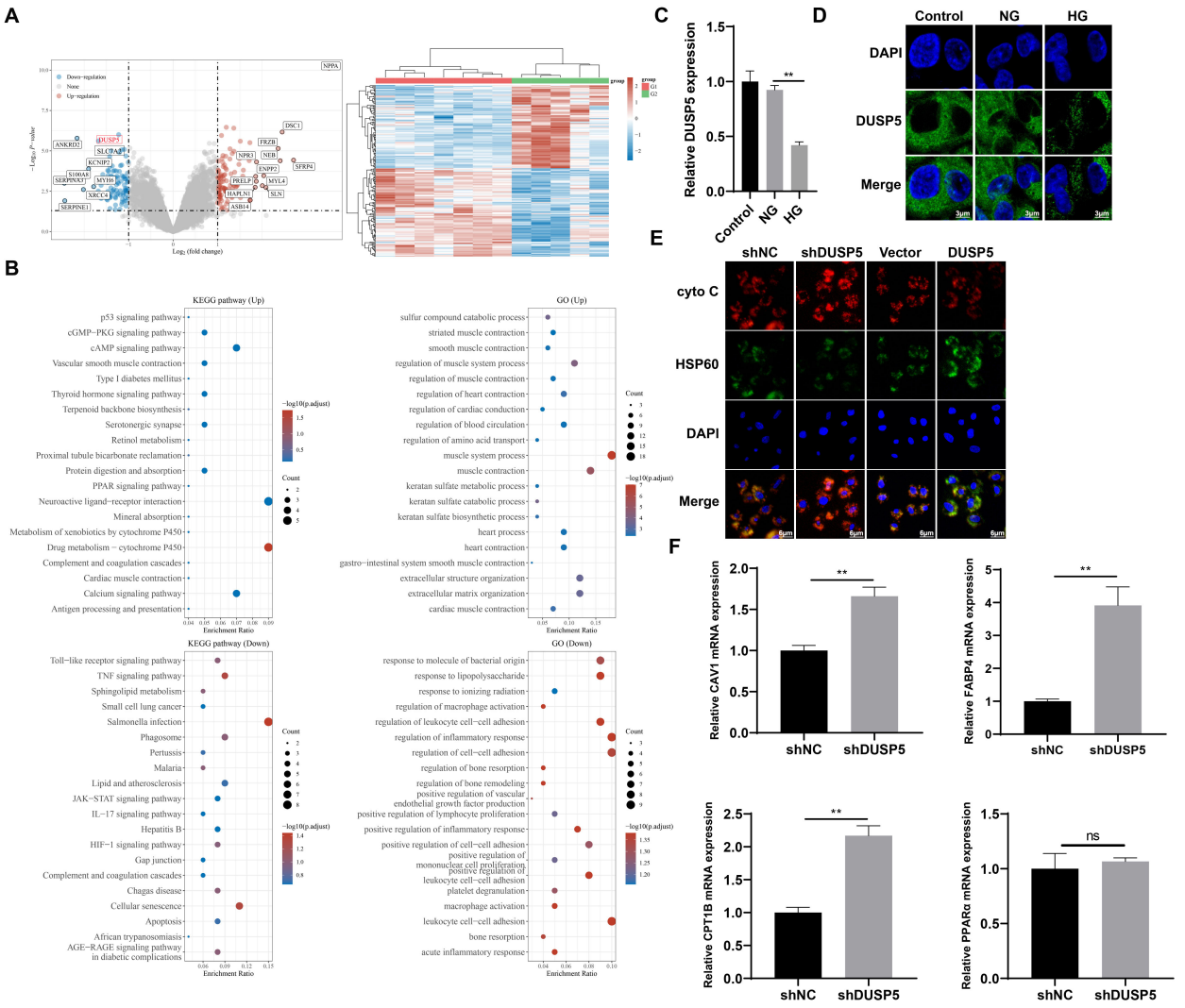

Fig. 1. *DUSP5* expression in diabetes-mediated heart failure. (A) Differentially expressed genes (DEGs) were analyzed using online microarray GSE26887. (B) The enrichment of DEGs was analyzed using KEGG and GO. (C) After exposed to HG, the mRNA expression of *DUSP5* was determined using qRT-PCR. N = 3. (D) After exposed to HG, *DUSP5* expression was determined using immunofluorescence. N = 3. (E) After exposed to HG, *HSP60* (red) and *cyto C* (green) expression was determined using immunofluorescence. N = 3. (F) The mRNA expression of fatty acid oxidation regulators was determined using qRT-PCR. N = 3. $^{**}p < 0.01$; ns, no significant difference. HG, high glucose; NG, normal glucose; shDUSP5, small hairpin RNA of *DUSP5*; NC, negative control; vector, empty vector; *DUSP5*, dual specificity phosphatase 5; KEGG, Kyoto Encyclopedia of Genes and Genomes; GO, Gene Ontology; cyto C, cytochrome C; HSP60, heat-shock protein 60; DAPI, 4′,6-diamidino-2-phenylindole.

showed that *PPARα* was mainly expressed in the nucleus ($p < 0.01$), which was downregulated by *DUSP5* overexpression.

PPARα Overexpression Promotes the Death of AC16 Cells

Cells were exposed to the PPARα agonists WY14643 and Fenofibrate (FEN). *PPARα* expression was increased by WY14643 ($p < 0.05$) and FEN ($p < 0.01$; Fig. 4A; **Supplementary Fig. 5**). FEN, which had more notable effects, was used in the subsequent experiment. As shown in Fig. 4B, FEN markedly increased the release of ROS and MDA. The apoptosis rates were also notably increased by FEN compared with those in the HG + *DUSP5* group ($p < 0.01$; Fig. 4C).

DUSP5 Overexpression Suppresses Diabetes-Mediated HF in Vivo

A diabetic rat model was established to verify the roles of *DUSP5* in diabetes-mediated HF. As shown in **Supplementary Fig. 6**, STZ injection contributed to HF. STZ injection significantly increased heart weight ($p <$

Journal of
BIOLOGICAL REGULATORS
and Homeostatic Agents

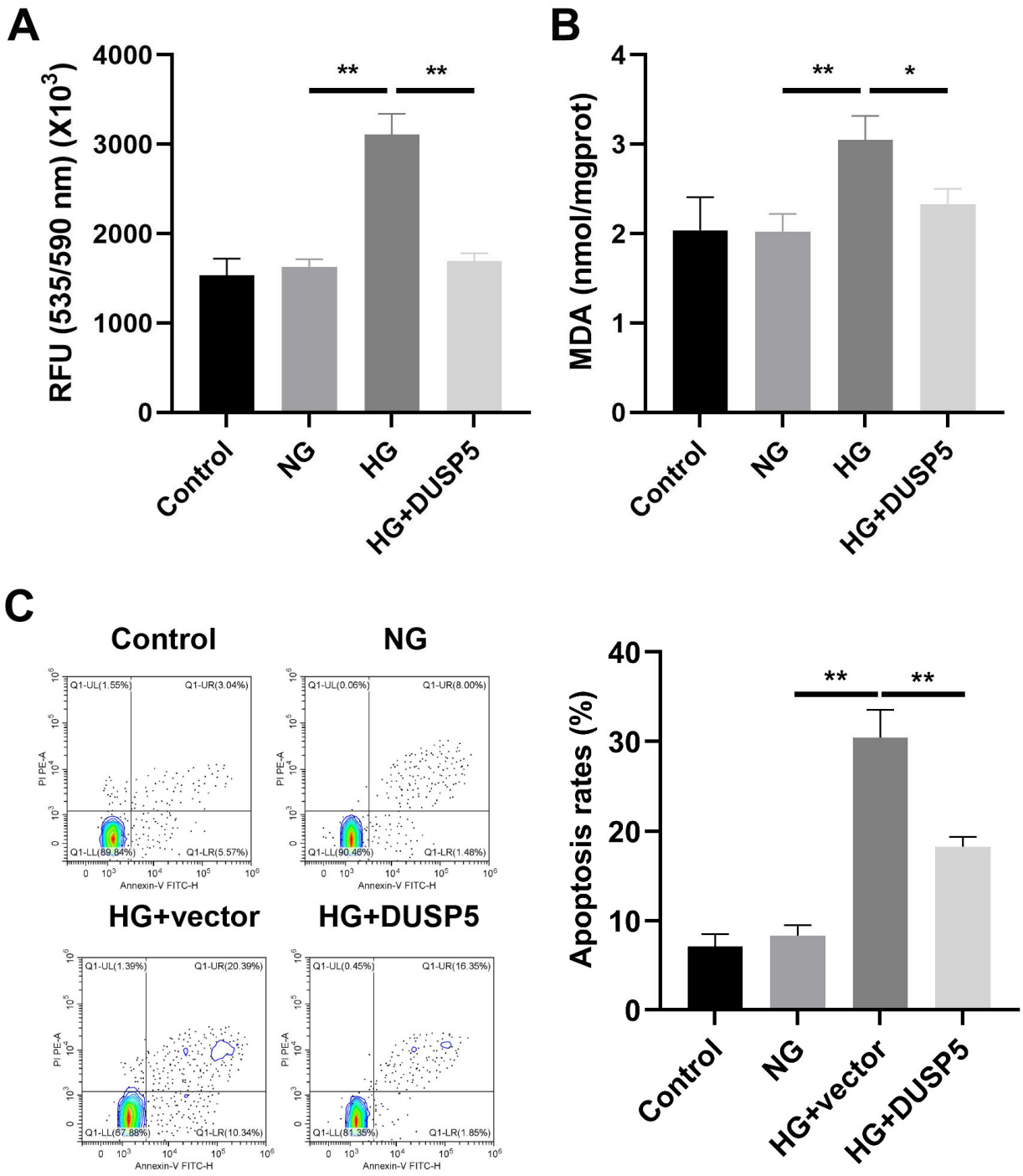

Fig. 2. *DUSP5* overexpression suppresses the apoptosis of cardiomyocytes. After transfected with *DUSP5* overexpression plasmids or the empty vector, ROS (A) and MDA. N = 3. (B) Release was determined. N = 3. (C) Cell apoptosis was determined by flow cytometry. N = 3. *$p < 0.05$, **$p < 0.01$. HG, high glucose; NG, normal glucose; vector, empty vector; *DUSP5*, dual specificity phosphatase 5; ROS, reactive oxygen species; MDA, malondialdehyde.

0.001; **Supplementary Fig. 6A,B**), and promoted the cell hypertrophic response ($p < 0.001$; **Supplementary Fig. 6C**) and the fibrotic response ($p < 0.001$; **Supplementary Fig. 6D**), suggesting that an *in vivo* model of diabetes-related HF was successfully established. TTC staining was performed to determine the infarct area. As shown in Fig. 5A, the infarct area was significantly increased by STZ ($p < 0.001$); however, this was significantly alleviated by *DUSP5* overexpression ($p < 0.01$). Moreover, *DUSP5* overexpression markedly decreased the amount of TUNEL-

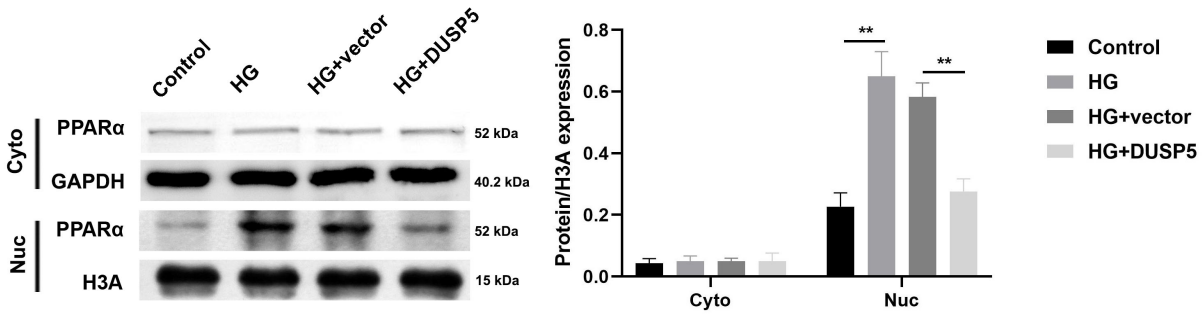

Fig. 3. DUSP5 suppresses the nuclear expression of PPARα. After transfected with DUSP5 overexpression plasmids or the empty vector, the protein expression of PPARα was determined by western blot. N = 3. $^{**}p < 0.01$. HG, high glucose; NG, normal glucose; vector, empty vector; DUSP5, dual specificity phosphatase 5; PPARα, peroxisome proliferator-activated receptor alpha; H3A, histone H3; GAPDH, glyceraldehyde-3-phosphate dehydrogenase.

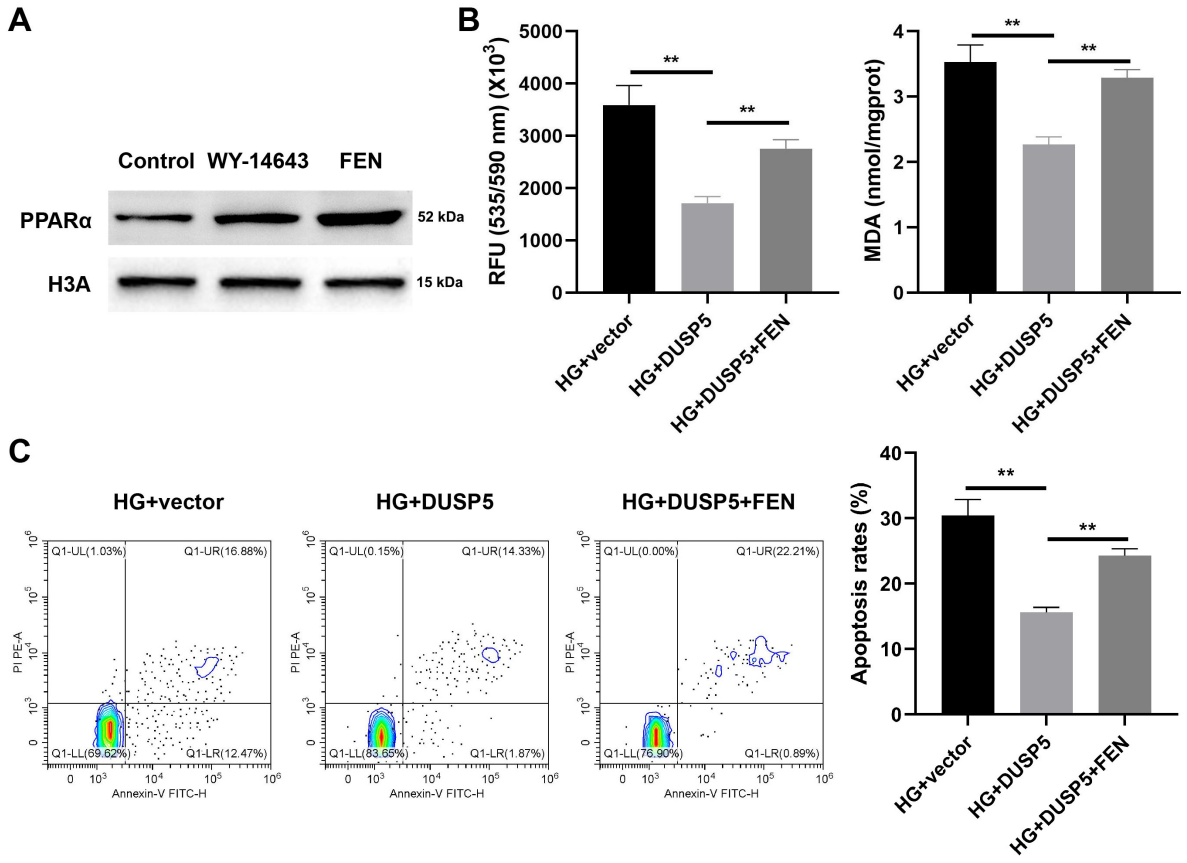

Fig. 4. *PPARα* overexpression promotes the death of cardiomyocytes. Cardiomyocytes were exposed to PPARα agonist WY14643 and FEN based on HG treatment. (A) The protein expression of PPARα determined by western blot. N = 3. (B) The ROS and MDA release was determined. N = 3. (C) Cell apoptosis was determined by flow cytometry. N = 3. $^{**}p < 0.01$. HG, high glucose; vector, empty vector; *DUSP5*, dual specificity phosphatase 5; FEN, Fenofibrate; ROS, reactive oxygen species; MDA, malondialdehyde; *PPARα*, peroxisome proliferator-activated receptor alpha; H3A, histone H3.

positive cells induced by STZ ($p < 0.001$; Fig. 5B). Additionally, STZ mediated an increase in *CAV1*, *FABP4* and *CPT1B*expression ($p < 0.01$, $p < 0.001$; Fig. 5C), whereas *DUSP5* overexpression decreased the expression of FAO-associated genes ($p < 0.01$).

DUSP5-NP Restore Heart Functions

MSCs are widely used in the treatment of CVD. Compared with the positive control, the results of qRT-PCR in rat MSCs showed no amplification (**Supplementary Fig. 4B**), suggesting that rat MSCs were not infected with *My-*

Journal of
BIOLOGICAL REGULATORS
and Homeostatic Agents

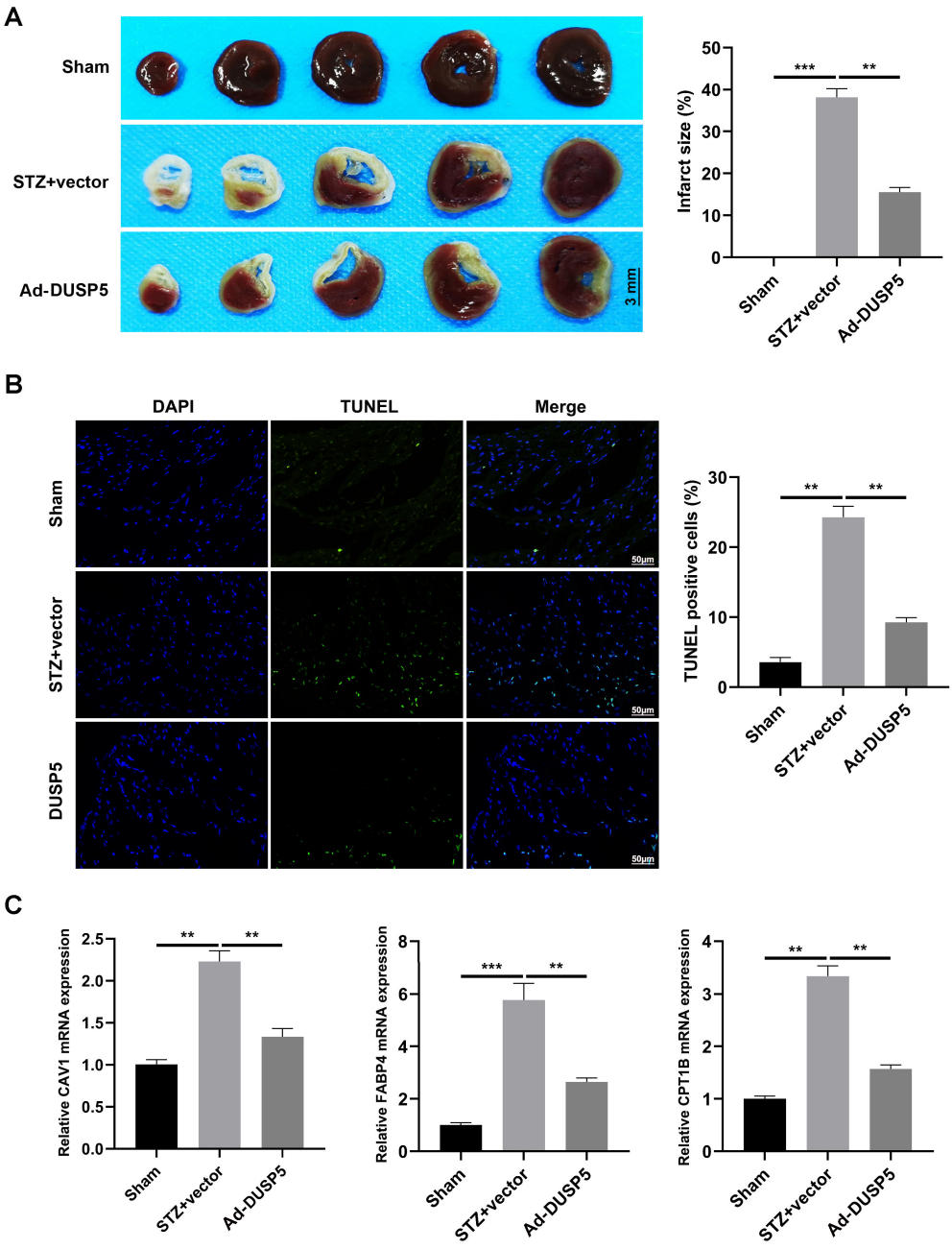

Fig. 5. *DUSP5* overexpression suppresses diabetes-mediated heart failure *in vivo*. Diabetic rat model was established by intravenously injecting with STZ. (A) TTC staining was performed to determine the infarct area. Scale bar = 3 mm. N = 6. (B) Cell death was analyzed using TUNEL assay. N = 6. (C) The expression of fatty acid oxidation regulators was determined by qRT-PCR. N = 6. $^{**}p < 0.01$, $^{***}p < 0.001$. STZ, streptozotocin; TTC, triphenyl tetrazolium chloride; TUNEL, terminal deoxynucleotidyl transferase (TdT)-mediated dUTP nick-end labeling; vector, empty vector; Ad-DUSP5, adenoviruses expressing rat DUSP5.

coplasma. Rat MSCs showed uniform morphology and spindle-shaped appearance, and were arranged in whorls (**Supplementary Fig. 7A**). Furthermore, flow cytometry demonstrated that almost all of the cells were positive for the classical MSC surface markers *CD106*, *CD29* and *CD44*, and negative for the hematopoietic lineage and endothelial marker *CD34* (**Supplementary Fig. 7B**), thus indicating that these cells were high-purity MSCs. Moreover, *Mycoplasma* detection showed that MSCs were not infected with *Mycoplasma* (**Supplementary Fig. 4B**). Subsequently, we constructed *DUSP5*-overexpressing MSCs, collected *DUSP5* exosomes and loaded them with the PPARα antagonist GW-6471 by cyclic extrusion to produce heart-targeted NP for drug delivery (Fig. 6A). TEM

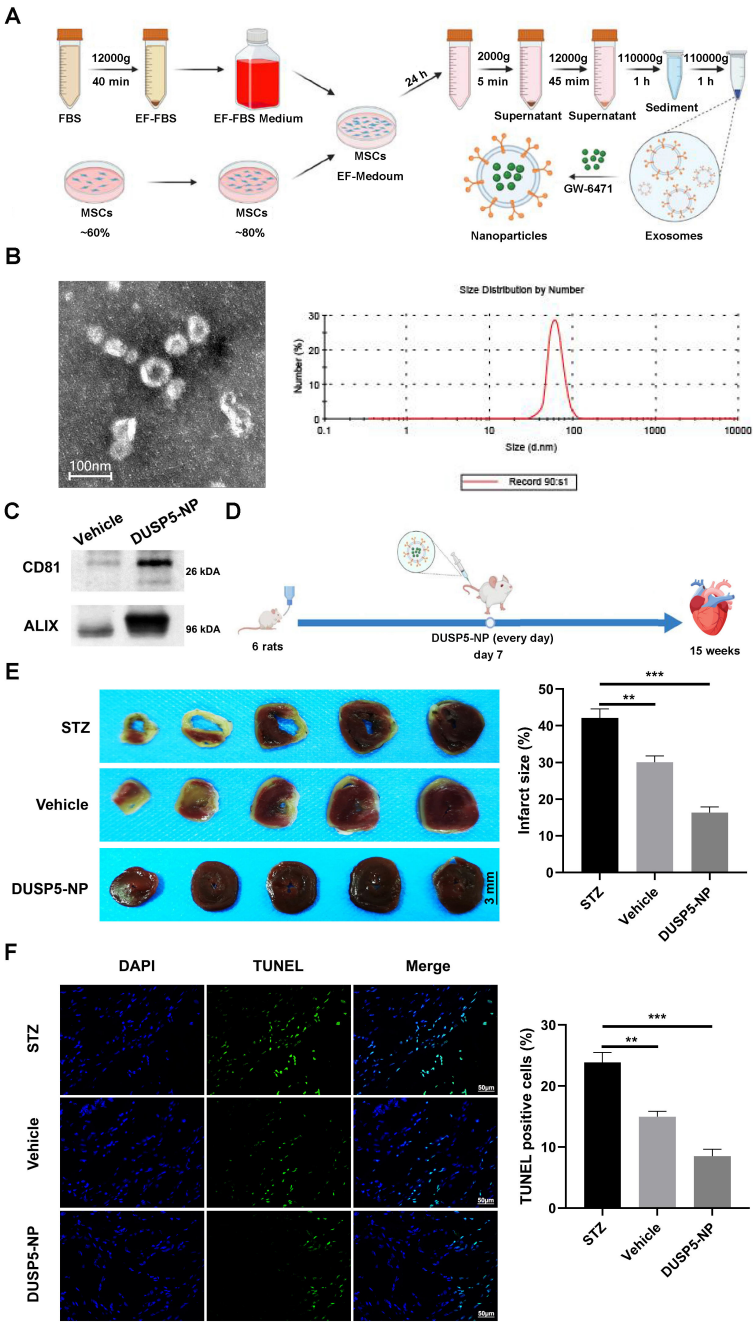

Fig. 6. DUSP5-NP restores heart functions. DUSP5-overexpressed MSCs were constructed. DUSP5 exosomes were harvested and loaded with PPARα antagonist (GW-6471) by cyclic extrusion to produce the heart-targeted NP for drug delivery. (A) Schematic diagram of exosome isolation. (B) The exosomes were pictured using transmission electron microscopy (TEM) and verified by nanoparticle tracking analysis (NTA). N = 6. (C) The protein expression of exosome markers (ALIX and CD81) was determined by western blot. N = 6. (D) Schematic diagram of diabetic rats treated by DUSP5-NP. N = 6. (E) TTC staining was performed to determine the infarct area. Scale bar = 3 mm. N = 6. (F) The death of cardiomyocytes determined using TUNEL assay. N = 6. $^{**}p < 0.01$, $^{***}p < 0.001$. STZ, streptozotocin; TTC, triphenyl tetrazolium chloride; TUNEL, terminal deoxynucleotidyl transferase (TdT)-mediated dUTP nick-end labeling; vehicle, DUSP5^{+} exosomes containing vehicle; DUSP5-NP, DUSP5^{+} exosomes loaded with PPARα antagonist GW-6471; ALIX, apoptosis-linked gene 2-interacting protein X; CD81, cluster of differentiation 81; MSCs, mesenchymal stem cell.

and NTA showed that the NP maintained the morphology of exosomes (Fig. 6B). Moreover, the protein expression of exosome markers, apoptosis-linked gene 2-interacting protein X and *CD81*, was significantly increased by *DUSP5* exosomes (Fig. 6C). The rats with diabetes-related HF were then injected with *DUSP5*-NP for 14 weeks. *DUSP5*$^{+}$ exo-

Journal of
BIOLOGICAL REGULATORS
and Homeostatic Agents

somes containing a vehicle served as the control (Fig. 6D). STZ treatment markedly decreased rat body weights ($p < 0.01$; **Supplementary Fig. 8**); however, the body weight of rats was increased following treatment with *DUSP5*-vehicle ($p < 0.05$) and *DUSP5*-NP ($p < 0.01$; **Supplementary Fig. 8**). Moreover, the body weight of rats in the *DUSP5*-NP group recovered to nearly that of the sham group compared with that in the vehicle group. Compared with the vehicle group ($p < 0.01$), *DUSP5*-NP had a more marked effect on decreasing the infarct area ($p < 0.001$; Fig. 6E). Moreover, compared with the vehicle group ($p < 0.01$), *DUSP5*-NP were more effective at suppressing cardiomyocyte death ($p < 0.001$; Fig. 6F).

Discussion

In this study, *DUSP5* was downregulated in diabetes-mediated HF. However, *DUSP5* overexpression suppressed the death of cardiomyocytes and FAO via inhibiting the nuclear translocation of *PPARα*. Moreover, *DUSP5* overexpression alleviated the infarct area *in vivo*. Additionally, *DUSP5*-NP improved heart functions with few side effects, suggesting that *DUSP5* may be a promising treatment strategy for diabetes-mediated HF.

Cardiomyocyte loss contributes to adverse remodeling and fibrosis, inevitably leading to HF [26]. The imbalance in cellular homeostasis induced by inflammation, oxidative stress, endoplasmic reticulum stress, metabolic stress, etc., plays a crucial role in the dysfunction of cardiomyocytes [27–29]. *PPARα* mediates the shift from anaerobic glycolysis to mitochondrial oxidative phosphorylation, and cardiac FAO results in the alteration of fatty acid utilization and transport, and cardiac dysfunction [10]. In diabetic cardiovascular cells, the increase in fatty acid flux and oxidation, in turn, stimulates the activation of *PPARα*, resulting in cardiomyopathy and HF. In this study, diabetes-mediated HF was accompanied by the stimulation of FAO. This is different from the HF induced by hypertension; myocardial FAO is stimulated in diabetes-mediated HF, whereas it is impaired in hypertension-induced HF, suggesting that pharmacological targeting of fatty acid metabolism may be considered a novel strategy to restore cardiac efficiency. Moreover, GW-6471 mediated overexpression of *PPARα* promoted the death of cardiomyocytes. However, GW-6471 (a PPARα antagonist) restored the heart functions *in vivo*, suggesting that inhibition of *PPARα* pathway-dependent cardiac FAO may be an alternative for diabetes-mediated HF.

DUSP5 is frequently found to be downregulated in heart diseases. Its dysfunction promotes the development of cardiac fibrosis, myocardial ischemia, T cell-mediated alloimmunity and diabetic cardiomyopathy [30–33]. These findings indicate that *DUSP5* may be involved in regulating mitochondrial oxidative metabolism in diabetes-mediated HF. In this study, *DUSP5* negatively regulated the expression of FAO-associated genes. Moreover, *DUSP5* promoted the translocation of *PPARα*, which dampens its functions in the activation of FAO. *DUSP5* was downregulated in diabetes-mediated HF. However, overexpression of *DUSP5* suppressed the death of cardiomyocytes and restored heart functions. Thus, *DUSP5*-mediated inhibition of *PPARα* signaling may provide a novel strategy for diabetes-mediated HF.

Exosome-based heart-targeted NP have been applied in the treatment of heart disorders [34]. Previous studies have revealed that exosome-liposome hybrid NP protect against ischemic-mediated HF, cardiomyocyte hypertrophy and chemotherapy-induced cardiotoxicity [35–37]. This suggests that exosomes may be used in precision medicine to treat heart disorders. In this study, we constructed *DUSP5*-NP to deliver GW-6471 (a PPARα antagonist). *DUSP5*-NP markedly suppressed FAO and alleviated heart infarction. Moreover, no side effects were found during treatment with *DUSP5*-NP, suggesting that anabolic therapy using MSC-derived exosomes may be promising in the future treatment of diabetes-mediated HF.

However, there are some limitations in this study. Firstly, the paper does not explore the regulatory mechanism of *DUSP5* expression in depth, such as what factors cause the downregulation of *DUSP5* in diabetes-related heart failure, and whether the overexpression or silencing of *DUSP5* affects the expression of other signaling pathways or genes. Secondly, the paper does not provide sufficient evaluation of the safety and efficacy of *DUSP5*-NP, such as the pharmacokinetics, pharmacodynamics, toxicology, immunogenicity and other aspects of *DUSP5*-NP.

Conclusions

In conclusion, *DUSP5* promoted the nuclear translocation of *PPARα* and inhibited FAO, which suppressed the death of cardiomyocytes and alleviated the heart infarction induced by diabetes-mediated HF. Identification of the *DUSP5-PPARα* interaction provides new perspectives for pharmacological interventions that target *PPARα*-mediated FAO in diabetes-mediated HF.

Availability of Data and Materials

The data used to support the findings of this study have been included in this article.

Author Contributions

JX contributed to the study conception and design. Material preparation, data collection and analysis were performed by CQ, JY, JG, and KW. The first draft of the manuscript was written by CQ. All authors contributed to editorial changes in the manuscript. All authors read and approved the final manuscript. All authors have participated sufficiently in the work and agreed to be accountable for all aspects of the work.

Ethics Approval and Consent to Participate

This study was approved by the Animal Care Broad of Nanjing Hospital Affiliated to Nanjing Medical University ([2022]027). The procedures of *in vivo* assays were performed in accordance with the Care and Use of Laboratory Animals published by the US National Institutes of Health.

Acknowledgment

Not applicable.

Funding

This research received no external funding.

Conflict of Interest

The authors declare no conflict of interest.

Supplementary Material

Supplementary material associated with this article can be found, in the online version, at https://doi.org/10.23812/j.biol.regul.homeost.agents.20243806.409.

References

[1] Meyer T, Shih J, Aurigemma G. In the clinic. Heart failure with preserved ejection fraction (diastolic dysfunction). Annals of Internal Medicine. 2013; 158: ITC5-ITC5-1-ITC5-15; quiz ITC5-16.

[2] Baman JR, Ahmad FS. Heart Failure. JAMA. 2020; 324: 1015.

[3] Marfella R, Sardu C, D'Onofrio N, Fumagalli C, Scisciola L, Sasso FC, *et al*. SGLT-2 inhibitors and in-stent restenosis-related events after acute myocardial infarction: an observational study in patients with type 2 diabetes. BMC Medicine. 2023; 21: 71.

[4] Nakamura K, Miyoshi T, Yoshida M, Akagi S, Saito Y, Ejiri K, *et al*. Pathophysiology and Treatment of Diabetic Cardiomyopathy and Heart Failure in Patients with Diabetes Mellitus. International Journal of Molecular Sciences. 2022; 23: 3587.

[5] Park JJ. Epidemiology, Pathophysiology, Diagnosis and Treatment of Heart Failure in Diabetes. Diabetes & Metabolism Journal. 2021; 45: 146–157.

[6] Karwi QG, Ho KL, Pherwani S, Ketema EB, Sun Q, Lopaschuk GD. Concurrent diabetes and heart failure: interplay and novel therapeutic approaches. Cardiovascular Research. 2022; 118: 686–715.

[7] Martín-Saladich Q, Simó R, Aguadé-Bruix S, Simó-Servat O, Aparicio-Gómez C, Hernández C, *et al*. Insights into Insulin Resistance and Calcification in the Myocardium in Type 2 Diabetes: A Coronary Artery Analysis. International Journal of Molecular Sciences. 2023; 24: 3250.

[8] Lee SE, Yoo J, Kim BS, Choi HS, Han K, Kim KA. The effect of metabolic dysfunction-associated fatty liver disease and diabetic kidney disease on the risk of hospitalization of heart failure in type 2 diabetes: a retrospective cohort study. Diabetology & Metabolic Syndrome. 2023; 15: 32.

[9] Lopaschuk GD, Karwi QG, Tian R, Wende AR, Abel ED. Cardiac Energy Metabolism in Heart Failure. Circulation Research. 2021; 128: 1487–1513.

[10] Fillmore N, Mori J, Lopaschuk GD. Mitochondrial fatty acid oxidation alterations in heart failure, ischaemic heart disease and diabetic cardiomyopathy. British Journal of Pharmacology. 2014; 171: 2080–2090.

[11] Zhou B, Tian R. Mitochondrial dysfunction in pathophysiology of heart failure. The Journal of Clinical Investigation. 2018; 128: 3716–3726.

[12] Yan Y, Li Q, Shen L, Guo K, Zhou X. Chlorogenic acid improves glucose tolerance, lipid metabolism, inflammation and microbiota composition in diabetic db/db mice. Frontiers in Endocrinology. 2022; 13: 1042044.

[13] Tao L, Huang X, Xu M, Qin Z, Zhang F, Hua F, *et al*. Value of circulating miRNA-21 in the diagnosis of subclinical diabetic cardiomyopathy. Molecular and Cellular Endocrinology. 2020; 518: 110944.

[14] Rahmatollahi M, Baram SM, Rahimian R, Saeedi Saravi SS, Dehpour AR. Peroxisome Proliferator-Activated Receptor-α Inhibition Protects Against Doxorubicin-Induced Cardiotoxicity in Mice. Cardiovascular Toxicology. 2016; 16: 244–250.

[15] Li Y, Xiong Z, Yan W, Gao E, Cheng H, Wu G, *et al*. Branched chain amino acids exacerbate myocardial ischemia/reperfusion vulnerability via enhancing GCN2/ATF6/PPAR-α pathway-dependent fatty acid oxidation. Theranostics. 2020; 10: 5623–5640.

[16] Liu X, Liu X, Du Y, Hu M, Tian Y, Li Z, *et al*. DUSP5 promotes osteogenic differentiation through SCP1/2-dependent phosphorylation of SMAD1. Stem Cells (Dayton, Ohio). 2021; 39: 1395–1409.

[17] Wu Z, Xu L, He Y, Xu K, Chen Z, Moqbel SAA, *et al*. DUSP5 suppresses interleukin-1β-induced chondrocyte inflammation and ameliorates osteoarthritis in rats. Aging. 2020; 12: 26029–26046.

[18] Yang Z, Huang D, Meng M, Wang W, Feng J, Fang L, *et al*. BAF53A drives colorectal cancer development by regulating DUSP5-mediated ERK phosphorylation. Cell Death & Disease. 2022; 13: 1049.

[19] Liu Y, Chen J, Liang H, Cai Y, Li X, Yan L, *et al*. Human umbilical cord-derived mesenchymal stem cells not only ameliorate blood glucose but also protect vascular endothelium from diabetic damage through a paracrine mechanism mediated by MAPK/ERK signaling. Stem Cell Research & Therapy. 2022; 13: 258.

[20] Tao H, Cao W, Yang JJ, Shi KH, Zhou X, Liu LP, *et al*. Long noncoding RNA H19 controls DUSP5/ERK1/2 axis in cardiac fibroblast proliferation and fibrosis. Cardiovascular Pathology: the Official Journal of the Society for Cardiovascular Pathology. 2016; 25: 381–389.

[21] Ferguson BS, Harrison BC, Jeong MY, Reid BG, Wempe MF, Wagner FF, *et al*. Signal-dependent repression of DUSP5 by class I HDACs controls nuclear ERK activity and cardiomyocyte hypertrophy. Proceedings of the National Academy of Sciences of the United States of America. 2013; 110: 9806–9811.

[22] Bogush N, Tan L, Naib H, Faizullabhoy E, Calvert JW, Iismaa SE, *et al*. DUSP5 expression in left ventricular cardiomyocytes of young hearts regulates thyroid hormone (T3)-induced proliferative ERK1/2 signaling. Scientific Reports. 2020; 10: 21918.

[23] Wu QQ, Yao Q, Hu TT, Wan Y, Xie QW, Zhao JH, *et al*. Tax1 banding protein 1 exacerbates heart failure in mice by activating ITCH-P73-BNIP3-mediated cardiomyocyte apoptosis. Acta Pharmacologica Sinica. 2022; 43: 2562–2572.

[24] Qi B, He L, Zhao Y, Zhang L, He Y, Li J, *et al*. Akap1 deficiency exacerbates diabetic cardiomyopathy in mice by NDUFS1-mediated mitochondrial dysfunction and apoptosis. Diabetologia. 2020; 63: 1072–1087.

[25] Sadeqi S, Nikkhahi F, Javadi A, Eskandarion S, Amin Marashi SM. Development of multiplex real-time quantitative PCR for simultaneous detection of Chlamydia trachomatis, Mycoplasma hominis, Ureaplasma urealyticum, and Mycoplasma genitalium

Journal of
BIOLOGICAL REGULATORS
and Homeostatic Agents

in infertile women. Indian Journal of Medical Microbiology. 2022; 40: 231–234.

[26] Wei X, Zou S, Xie Z, Wang Z, Huang N, Cen Z, *et al*. EDIL3 deficiency ameliorates adverse cardiac remodelling by neutrophil extracellular traps (NET)-mediated macrophage polarization. Cardiovascular Research. 2022; 118: 2179–2195.

[27] Forrester SJ, Kikuchi DS, Hernandes MS, Xu Q, Griendling KK. Reactive Oxygen Species in Metabolic and Inflammatory Signaling. Circulation Research. 2018; 122: 877–902.

[28] Rius-Pérez S, Torres-Cuevas I, Millán I, Ortega ÁL, Pérez S. PGC-1α, Inflammation, and Oxidative Stress: An Integrative View in Metabolism. Oxidative Medicine and Cellular Longevity. 2020; 2020: 1452696.

[29] Kyriazis ID, Hoffman M, Gaignebet L, Lucchese AM, Markopoulou E, Palioura D, *et al*. KLF5 Is Induced by FOXO1 and Causes Oxidative Stress and Diabetic Cardiomyopathy. Circulation Research. 2021; 128: 335–357.

[30] Tao H, Yang JJ, Hu W, Shi KH, Deng ZY, Li J. MeCP2 regulation of cardiac fibroblast proliferation and fibrosis by down-regulation of DUSP5. International Journal of Biological Macromolecules. 2016; 82: 68–75.

[31] Zeng M, Wei X, He YL, Chen JX, Lin WT, Xu WX. EGCG protects against myocardial I/RI by regulating lncRNA Gm4419-mediated epigenetic silencing of the DUSP5/ERK1/2 axis. Toxicology and Applied Pharmacology. 2021; 433: 115782.

[32] Pan G, Zhang J, Han Y, Chen Y, Guo X, Cui X, *et al*. CX-5461 is a potent immunosuppressant which inhibits T cell-mediated alloimmunity via p53-DUSP5. Pharmacological Research. 2022; 177: 106120.

[33] Xu Z, Tong Q, Zhang Z, Wang S, Zheng Y, Liu Q, *et al*. Inhibition of HDAC3 prevents diabetic cardiomyopathy in OVE26 mice via epigenetic regulation of DUSP5-ERK1/2 pathway. Clinical Science (London, England: 1979). 2017; 131: 1841–1857.

[34] Stine SJ, Popowski KD, Su T, Cheng K. Exosome and Biomimetic Nanoparticle Therapies for Cardiac Regenerative Medicine. Current Stem Cell Research & Therapy. 2020; 15: 674–684.

[35] Liu S, Chen X, Bao L, Liu T, Yuan P, Yang X, *et al*. Treatment of infarcted heart tissue via the capture and local delivery of circulating exosomes through antibody-conjugated magnetic nanoparticles. Nature Biomedical Engineering. 2020; 4: 1063–1075.

[36] Liu Q, Piao H, Wang Y, Zheng D, Wang W. Circulating exosomes in cardiovascular disease: Novel carriers of biological information. Biomedicine & Pharmacotherapy = Biomedecine & Pharmacotherapie. 2021; 135: 111148.

[37] Sun W, Zhao P, Zhou Y, Xing C, Zhao L, Li Z, *et al*. Ultrasound targeted microbubble destruction assisted exosomal delivery of miR-21 protects the heart from chemotherapy associated cardiotoxicity. Biochemical and Biophysical Research Communications. 2020; 532: 60–67.